Modification of Oligosaccharide Antenna Flexibility Induced by Exoglycosidase Trimming†

Kevin G. Rice,‡ Pengguang Wu,§ Ludwig Brand,§ and Yuan C. Lee*,§

Department of Biology, Johns Hopkins University, Baltimore, Maryland 21218, and Division of Pharmaceutics and Pharmaceutical Chemistry, College of Pharmacy, The Ohio State University, Columbus, Ohio 43210

Received December 29, 1992; Revised Manuscript Received April 19, 1993

ABSTRACT: We have investigated the solution conformation of a triantennary glycopeptide using resonance energy transfer [Rice et al. (1991) *Biochemistry 30*, 6646–6655]. Triantennary glycopeptide was derivatized with a donor fluorophore on the N-terminus and with an acceptor fluorophore attached individually to each terminal galactose residue, resulting in three isomeric donor–acceptor pairs. Time-resolved energy-transfer experiments revealed two distinct donor–acceptor distance populations for two of the three antennae of the oligosaccharide. An extended conformation and a folded conformation were detected for the two flexible antennae whereas the third antenna on the oligosaccharide was rigid, containing only an extended conformer. The ratios of the extended to folded conformers of the two flexible antennae were reversibly modulated by temperature, allowing the calculation of ΔH and ΔS for the conformational change [Wu et al. (1991) *Proc. Natl. Acad. Sci. U.S.A. 88*, 9355–9359]. In the present study, we have trimmed the fluorescent glycopeptides with exoglycosidases which specifically removed the unmodified antennae of the oligosaccharide. The resulting single-chain isomeric glycopeptides each contained identical core sugar residues and a terminally located donor and acceptor, but differed only in the linkage configuration of the sugar residues. Analysis of these glycopeptides by time-resolved energy transfer indicated that each antenna of the oligosaccharide is, by itself, maintained exclusively in the extended conformation. Temperature modulation failed to induce antenna folding as was previously observed for the complete triantennary structure. These data suggest that interantenna interactions modulate the conformation of individual antenna of complex oligosaccharides.

Complex oligosaccharides are components of glycoprotein receptors, hormones, and enzymes. They may function in transporting glycoproteins for cellular uptake mediated through binding to endogenous lectins (Kornfeld & Kornfeld, 1985). The degree of the interaction between complex oligosaccharides and mammalian lectins depends on the topography of binding sites on the lectin and the three-dimensional arrangement of "target" residues on the oligosaccharide (Lee, 1989). However, complex oligosaccharides are not completely rigid in solution. Previous studies have concluded that the antenna can assume numerous conformations based on the flexibility of glycosidic linkages (Bock et al., 1982; Cumming et al., 1987; Homans et al., 1987).

The functional significance of conformational heterogeneity in complex oligosaccharides has not been established. In "docking" of the multivalent oligosaccharide to a lectin, antenna flexibility allows proper alignment of target residues on the ligand with multiple binding pockets on the receptor. The protein to which oligosaccharides are linked may influence the conformation of N-linked oligosaccharides, and thus the peptide portion of a glycoprotein may exert some control over the binding interaction.

We have previously analyzed the solution conformation of a triantennary glycopeptide which is a high-affinity ligand for the rat hepatic lectin (Rice et al., 1990; Townsend et al., 1986). We found a correlation between antenna flexibility on the oligosaccharide and the binding geometry of this ligand to the lectin (Rice & Lee, 1992). Flexible antennae on triantennary oligosaccharide predispose two of the terminal galactose residues to combine at a high frequency with binding sites on the major subunit of the rat hepatic lectin whereas the third antenna is rigid and positions the remaining galactose residue for binding to the minor receptor subunit (Rice et al., 1990). These results have focused our attention to further investigate interactions in the triantennary ligand which control the equilibrium between extended and folded conformations of flexible antennae.

Most studies have analyzed the conformation of N-linked oligosaccharides or their component oligosaccharide segments using NMR nuclear Overhauser effect (NOE) as the primary tool to provide data for molecular modeling (Homans, 1990; Poppe et al., 1992; Edge et al., 1990). Recently, we have introduced resonance energy transfer as an alternative approach to analyze the conformation of complex glycopeptides (Rice et al., 1991; Wu et al., 1991). Resonance energy transfer has the advantage of providing long-range intramolecular distances in addition to directly measuring the distribution of distance populations in flexible polymers such as oligosaccharides.

Our initial investigation established the feasibility of selectively derivatizing a triantennary glycopeptide with a donor fluorophore on the peptide N-terminus and an acceptor fluorophore attached individually to each terminal galactose residue of the oligosaccharide (Rice & Lee, 1990). Time-resolved energy-transfer experiments identified both an extended and a folded conformer for two of the three antennae on the triantennary glycopeptide (Rice et al., 1991). The ratio of these conformers on the flexible antennae was reversibly modulated by temperature (Wu et al., 1991). These studies indicate the existence of multiple sites of flexibility in the triantennary glycopeptide. However, factors that dictate the distribution of conformational isomers remain unknown. Whether an antenna adopts a folded or extended conformation depends not only on its intrinsic flexibility but also on its

† This work was supported by National Institutes of Health Research Grants GM48049 (K.G.R.), DK09970 (Y.C.L.), and GM11632 (P.W. and L.B.).

* To whom correspondence should be addressed.

‡ The Ohio State University.

§ Johns Hopkins University.

0006-2960/93/0432-7264$04.00/0

interaction with other antenna in the same molecule and on the solution conditions.

In the present study, we have probed conformational changes in triantennary glycopeptide in response to oligosaccharide structure modification with exoglycosidases. The results of this study demonstrate the unique capabilities of energy transfer to detect subtle changes in oligosaccharide conformation. These experiments may lead to a more detailed understanding of the relationship between the primary structure of an oligosaccharide and its conformation.

MATERIALS AND METHODS

Chromatography was performed on a Gilson gradient HPLC equipped with an ISCO V4 UV/Vis variable-wavelength detector, a Perkin-Elmer LS40 scanning fluorescence detector, and an HP Inkjet integrator. All HPLC columns were purchased from Phase Separation, Norwalk, CT. β-Galactosidase (EC 3.2.1.23) and β-*N*-acetylglucosaminidase (EC 3.2.1.30) were purchased from Boehringer Mannheim, Indianapolis, IN. α-Mannosidase (EC 3.2.1.24) was purchased from V-Labs, Covington, LA. 2-Naphthylacetic acid, *N*-hydroxysuccinimide, and dicyclohexylcarbodiimide were purchased from Aldrich Chemical Co., Milwaukee WI. Mono-*N*-dansylethylenediamine was obtained from Molecular Probes Inc., Eugene, OR.

Fluorescent Labeling of Triantennary Glycopeptide. The preparation of triantennary glycopeptides containing a donor and an acceptor fluorophore has been described (Rice & Lee, 1990). Briefly, 2-naphthylacetic acid was activated as an ester of *N*-hydroxysuccinimide and coupled to the N-terminus of triantennary glycopeptide. The derivatized glycopeptide was used as a substrate for galactose oxidase. Partial oxidation resulted in the isolation of each isomeric monooxoglycopeptide which was distinguished by proton NMR. Mono-*N*-dansylethylenediamine was attached to the terminal 6-oxogalactose on each glycopeptide isomer by reductive amination. Each doubly labeled glycopeptide chromatographed as a single peak eluting later than the glycopeptides containing either dansyl or naphthyl groups. Therefore, the labeling of the glycopeptides with acceptor probe was considered to be quantitative. Each of the fluorescent glycopeptides was characterized by steady-state and time-resolved fluorescence energy transfer (Rice et al., 1991).

Enzymatic Modification of Triantennary Glycopeptide. The fluorescently labeled triantennary glycopeptides (600 nmol) were dissolved in 200 μL of buffer (0.1 M citrate phosphate, pH 4.3), and 50 milliunits of β-galactosidase was added and allowed to react for 24 h at 37 °C. The reaction progress was monitored by injecting 1 μL of the sample onto an octyl (0.47 × 25 cm) column being eluted at 1 mL/min with 10 mM ammonium acetate, pH 5.0, and a gradient of acetonitrile (0 time, 10%; 7 min, 10%; 15 min, 18%; 40 min, 27%; 50 min, 27%). At completion of the reaction, 2.5 units of β-*N*-acetylglucosaminidase (5 μL) was added and incubated for an additional 24 h at 37 °C. Finally, 2 units of α-mannosidase was added to each glycopeptide isomer and reacted at 37 °C for an additional 24 h. The glycopeptide products were preparatively isolated from the analytical RP-HPLC column, detecting eluting peaks by A_{220nm}. The major exoglycosidase product (95%) from each isomer was collected and freeze-dried.

Characterization of Fluorescent Glycopeptides. Each glycopeptide product was characterized by monosaccharide compositional analysis and by proton NMR. The purified glycopeptides (1 nmol) were dissolved in 200 μL of 2 N trifluoroacetic acid and hydrolyzed at 100 °C for 4 h. The acid was removed under a Speed-Vac evaporator. The samples were reconstituted into 200 μL of water, and 100 μL was analyzed by high-pH anion-exchange chromatography (HPAEC) comparing the peak area and retention time to appropriate monosaccharide standards (Hardy et al., 1988).

Glycopeptides were prepared for NMR by repeated freeze-drying in D_2O. The D_2O-exchanged sample was prepared in 200 μL of D_2O containing acetone as an internal standard. The proton NMR spectra were acquired on a Bruker 500-MHz spectrophotometer.

Steady-State and Time-Resolved Resonance Energy Transfer. Steady-state fluorescence energy transfer was performed using a microanalytical HPLC experiment as previously described (Rice et al., 1991). An equimolar sample containing naphthylacetylglycopeptide, three substrate triantennary glycopeptides, and three product glycopeptides was prepared (see Figure 1 for structures). In three consecutive chromatograms, this sample was resolved into component peaks by RP-HPLC in which only the mode of detection was changed. Fluorescence detection was specific for naphthyl (excitation 280 nm, emission 340 nm) or dansyl (excitation 334 nm, emission 520 nm). The absorbance at 220 nm was also used to detect the eluting peaks to correct for the relative concentrations.

Time-resolved fluorescence was performed using a single photon counting apparatus with a picosecond synchronously pumped mode-locked dye laser as described elsewhere (Badea & Brand, 1979; Wu et al., 1991). Naphthyl-2-acetyl was excited at 290 nm, and its emission was detected at 350 nm. The instrument response was about 60 ps. Duplicate or triplicate data were collected at 1, 20, and 40 °C. Samples were prepared in 2 mM sodium phosphate, pH 7.2.

The donor decay in the absence of acceptor was analyzed by a sum of exponentials:

$$I_D(t) = \sum_i \alpha_i \exp\left(-\frac{t}{\tau_i}\right) \quad (1)$$

The goodness of fit was judged by the reduced χ^2, the weighted residuals, and the autocorrelation of the residuals (Grinvald & Steinberg, 1974). This allowed determination of the α_i and τ_i values for the donor in the absence of acceptor at each temperature.

The fluorescence decay curve for the glycopeptide products was fit to eq 2 by nonlinear least-squares analysis to determine the distribution (P):

$$I_{DA}(t) = \int P(r) \sum_{i=1}^{n} \alpha_i \exp\left[-\frac{t}{\tau_i}\left(1 + \left(\frac{R_0}{r}\right)^6\right)\right] dr \quad (2)$$

where R_0 is the Förster distance calculated using $\kappa^2 = 2/3$. We used a Lorentzian distance distribution function in the fit (Rice et al., 1991)

$$P(r) = \frac{1}{\sigma\pi} \frac{1}{1 + ([(r - \bar{r})/\sigma]^2)} \quad (3)$$

where $\bar{r}$ is the mean distance and σ is the standard deviation of the distribution. In the case of an asymmetric distance distribution, a parameter of asymmetry was included as before (Wu & Brand, 1992).

RESULTS

Preparation and Characterization of Fluorescent Glycopeptides. Three isomeric fluorescent triantennary glycopeptides, containing a donor and a uniquely located acceptor, were used as substrates for exoglycosidases (Figure 1,

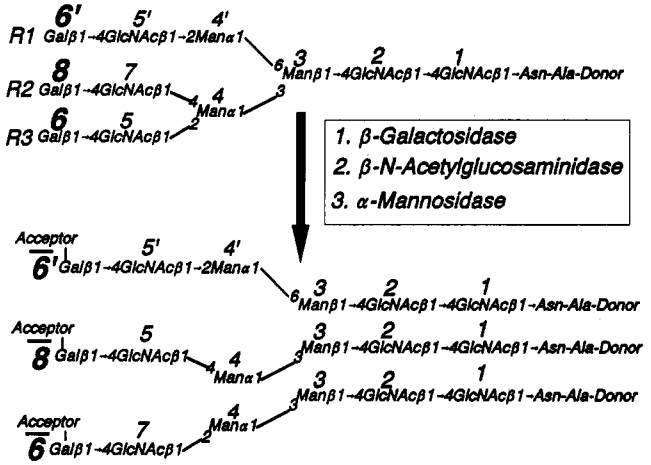

FIGURE 1: Exoglycosidase reaction scheme. The structures of glycopeptide substrates (**6**, **8**, and **6′**) and products ($\bar{6}$, $\bar{6'}$, and $\bar{8}$) are shown where R1, R2, and R3 indicate the location of the single dansyl group resulting in three geometric isomers. The structures are identified according to the number of the galactose residue to which the dansyl group is linked.

Table I

compound[a]	GlcNAc[b]	mannose[b]	galactose[b]
naphthyl-GP	3.5	2.3	2.8
6	3.3	2.3	2.0
6′	3.7	2.3	2.1
8	3.2	2.3	1.9
$\bar{6}$	1.7	2	ND[c]
$\bar{6'}$	1.8	2	ND
$\bar{8}$	1.5	2	ND

[a] See Figure 1 for the structure of each isomer. [b] Determined by trifluoroacetic acid (TFA) hydrolysis. [c] Not detected.

compounds **6**, **8**, and **6′**). Modification of galactose at C-6 with mono-*N*-dansylethylenediamine provided resistance to cleavage by β-galactosidase. Consequently, the products of this and subsequent enzyme reactions still contained both fluorophores.

β-*N*-Acetylglucosaminidase and α-mannosidase removed the exposed GlcNAc and mannose residues from the degalactosylated antenna. In each case, the removal of sugar residues by exoglycosidases resulted in a shift to longer retention times on RP-HPLC.

The resulting products (Figure 1, compounds $\bar{8}$, $\bar{6}$, and $\bar{6'}$) were characterized by monosaccharide compositional analysis and high-field proton NMR. Monosaccharide analysis indicated the complete loss of galactose from the product glycopeptides even though a single galactose residue remained as part of the structure. This is because the remaining galactose was altered with dansyl and no longer eluted coincidentally with a galactose standard on HPAEC. The hydrolysate of each product glycopeptide showed nearly a 2:2 ratio of mannose/GlcNAc compared to the triantennary glycopeptide substrates which provided a ratio of approximately 2:2.3:3.3 for galactose/mannose/GlcNAc (Table I). As has been documented before (Hardy et al., 1988; Rice et al., 1992), the theoretical ratio of 3:2 of mannose/GlcNAc was not observed from the hydrolyzate of each glycopeptide, because of the slower hydrolysis of the GlcNAc–Asn linkage under the hydrolytic conditions employed.

Proton NMR was used to establish the identity of the exoglycosidase products (Figure 2). In agreement with the proposed structures, each isomeric product contained only three GlcNAc CH_3CO resonances between 2.1 and 1.9 ppm,

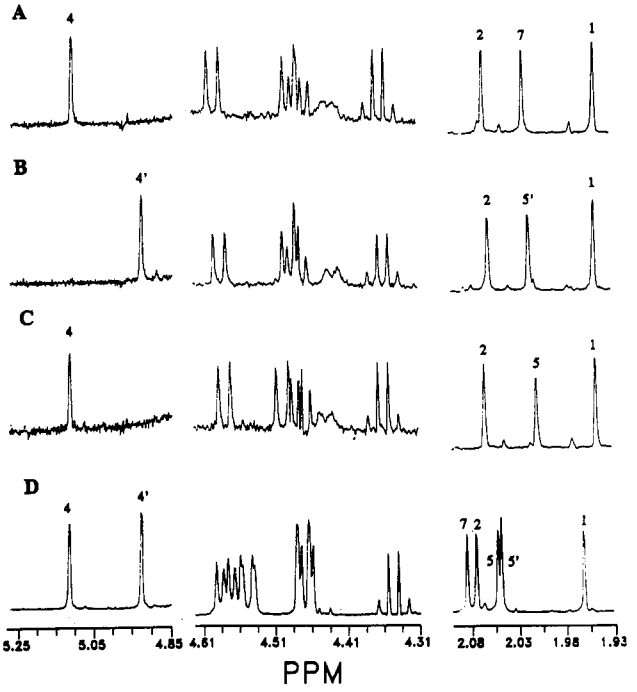

FIGURE 2: Partial 500-MHz proton NMR spectra of glycopeptide products ($\bar{6}$, $\bar{6'}$, and $\bar{8}$) and naphthyl triantennary glycopeptide (panels A–D, respectively). The mannose anomeric region (5.3–4.85 ppm), the galactose and GlcNAc anomeric region (4.65–3.31 ppm), and the GlcNAc *N*-acetyl region (2.1–1.93 ppm) are illustrated. The spectra were acquired at 23 °C in D_2O containing acetone as the internal standard. The resonance assignments refer to sugar residues designated in Figure 1.

compared with the naphthylacetyl triantennary glycopeptide which had five. The acetyl and methyl signals are tentatively assigned as GlcNAc 1, 2, 5, 5′, and 7 as shown (Figure 2A–D) based on a comparison of their chemical shifts with similar resonances in triantennary glycopeptide.

The NMR spectra of each isomeric product contained only a single mannose anomeric resonance between 5.2 and 4.8 ppm (Figure 2A–C) compared with the spectra for naphthylacetyl triantennary glycopeptide which had resonances for both α-linked mannose residues (Figure 2D). These mannose anomeric resonances had identical chemical shifts relative to the Man 4 and 4′ residues in the naphthyl triantennary glycopeptide. Therefore, their assignment as either Man 4 or Man 4′ in $\bar{6}$, $\bar{6'}$, and $\bar{8}$ was unequivocal.

As anticipated, the $\bar{8}$ and $\bar{6}$ isomers each contained exclusively the Man 4 residue while the $\bar{6'}$ isomer contained only the Man 4′ residue. This result allowed assignment of the GlcNAc 5′-methyl signal in $\bar{6'}$ (Figure 2B). However, the NMR spectra could not unequivocally distinguish between $\bar{6}$ and $\bar{8}$. Both had signals with distinctive chemical shifts for GlcNAc and Gal residues, but a conclusive assignment for the location of the acceptor fluorophore could not be made from these data alone. Therefore, the location of dansyl in $\bar{8}$ and $\bar{6}$ is proposed on the basis of the location of the aldehyde group used for coupling, which was determined by proton NMR analysis of the monooxo triantennary glycopeptide isomers (Rice & Lee, 1990). In addition to resonances associated with the carbohydrate portion, each product contained resonances consistent with the Asn-Asp peptide and the dansyl and naphthyl group (not shown).

Steady-State and Time-Resolved Energy-Transfer Experiments. The $\bar{8}$, $\bar{6}$, and $\bar{6'}$ glycopeptides were readily resolved on RP-HPLC (Figure 3, panel A, 43–46 min). Each eluted approximately 8–10 min later than the triantennary

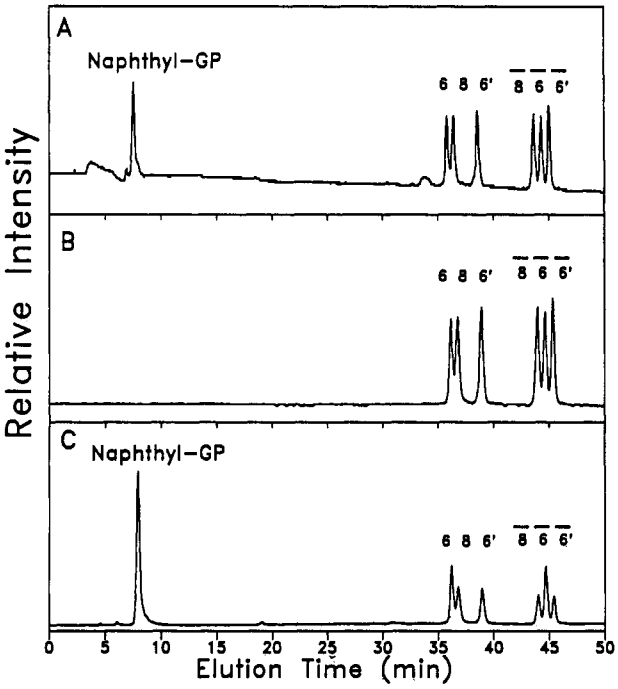

FIGURE 3: RP-HPLC separation of admixtures of naphthyl triantennary glycopeptide, fluorescent triantennary glycopeptides (**6**, **8**, and **6'**), and exoglycosidase-trimmed glycopeptides ($\bar{6}$, $\bar{6'}$, and $\bar{8}$). The separations were performed on an octyl reverse-phase column as described under Materials and Methods, detecting the eluting peaks by ether A_{220nm} (A), dansyl fluorescence (excitation 334 nm, emission 520 nm) (B), or naphthyl fluorescence (excitation 280 nm, emission 340 nm) (C).

glycopeptide substrates (**6**, **8**, and **6'**). However, $\bar{6}$, and $\bar{8}$ reversed their elution order relative to their respective parent compounds. Steady-state energy-transfer experiments were performed using an HPLC fluorometer as described previously (Rice et al., 1991). Detection of the eluting peaks by the absorbance at 220 nm preferentially measured the naphthyl chromophore, allowing normalization of the integration area based on molarity (Figure 3A). Fluorescence detection at an excitation wavelength of 334 nm and an emission wavelength of 520 nm measured dansyl and confirmed the relative molar concentration of the dansyl-containing glycopeptides (Figure 3B). Fluorescence detection with excitation of 280 nm and emission at 340 nm detected the naphthylacetyl group under donor quenching conditions (Figure 3C). However, the naphthylacetyl group fluorescence was differentially quenched in each isomer. The integration area for each glycopeptide substrate and product in Figure 3C was used to calculate the efficiency by

$$E = 1 - \left(\frac{F^{DA}}{F^{D}}\right) \tag{4}$$

where F^{DA} is the concentration-normalized integration area for glycopeptides containing both donor and acceptor and F^{D} is the integration area for the naphthyl glycopeptide. The efficiency was used to calculate the steady-state donor–acceptor distance according to

$$\bar{r} = R_0\left(\frac{1-E}{E}\right)^{1/6} \tag{5}$$

utilizing an R_0 value of 20.8 Å as previously determined (Rice et al., 1991). Under the solution conditions in HPLC, each product glycopeptide displayed a marginal decrease in the donor–acceptor distance compared with the fluorescent glycopeptide substrates (Table II). However, the donor–acceptor distances in triantennary glycopeptide substrates were identical to those reported previously (Rice et al., 1991). Equation 5 was used to obtain the average distance between donnor and acceptor. As has been shown elsewhere, calculation of average distances using an orientation factor of $^2/_3$ is reliable, and errors in the calculation generally do not exceed 10% (Wu & Brand, 1992).

Table II

compound[a]	efficiency, $\langle E\rangle$[b] (%)	donor–acceptor distance, $\langle r\rangle$[c] (Å)
6	45	21.5
$\bar{6}$	54	20.2
8	69	18.2
$\bar{8}$	78	16.8
6'	75	17.3
$\bar{6'}$	81	16.2

[a] See Figure 1 for the structure of each isomer. [b] Determined by donor quenching (Figure 3) using eq 1. [c] Steady-state distance determined using eq 2, where R_0 was 20.8 Å as previously determined for this donor and acceptor (Rice et al., 1991).

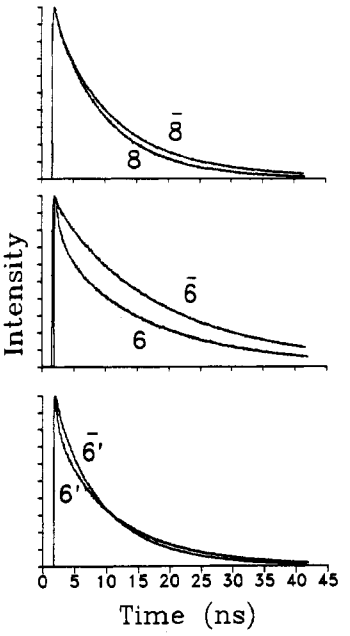

FIGURE 4: Comparison of donor fluorescence decay. The decay curves for **8**, **6**, and **6'** are compared with those for $\bar{8}$, $\bar{6}$, and $\bar{6'}$ at 20 °C. The curves were all normalized at peak position.

The removal of two antennae from the modified triantennary glycopeptides eliminates some possible steric interaction for the remaining antennae. It is thus interesting to directly compare the decay characteristics of the donor in the glycopeptide substrates (**6**, **8**, **6'**) with those in the product glycopeptides ($\bar{6}$, $\bar{8}$, $\bar{6'}$) using time-resolved energy transfer. Figure 4 illustrates the donor decays in glycopeptide substrates and products at 20 °C. The decay profiles of the donor in **8** and $\bar{8}$ are very similar even though $\bar{8}$ has a slightly longer decay time. Conversely, comparison of the donor's decay for **6** with $\bar{6}$ and for **6'** with $\bar{6'}$ demonstrates a large change. Since the local environment of the donor itself is the same, the shift in the decay characteristics is due to changes in quenching as a consequence of altered donor–acceptor distances. The most notable change occurs in the early part of the decay of $\bar{6}$ and $\bar{6'}$ relative to **6** and **6'**. These short decay times arise from a close approach of the donor to the acceptor (Rice et al., 1991; Wu et al., 1991). The loss of this decay rate in $\bar{6}$ and $\bar{6'}$ implies the disappearance of the folded conformation. We are able to reproducibly determine small changes in these

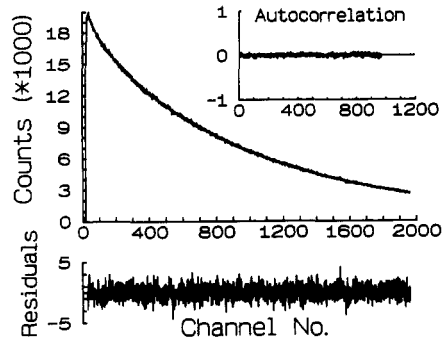

FIGURE 5: Donor decay fitting. The measured and fit decay data are shown for $\bar{6}$ at 1 °C. The intensity as counts is plotted versus the channel as time (11 ps per channel). The weighted residuals are plotted at the bottom, and the autocorrelation of the residuals is shown in the insert.

decay rates by sampling 1000–2000 data points for a single decay curve, which should be sufficient to base our statistical analyses.

The donor decay for $\bar{8}$, $\bar{6}$, and $\overline{6'}$ was analyzed by eq 2 using a Lorentzian model function. A typical fit for the $\bar{6}$ isomer is shown in Figure 5. A single distance population is adequate to describe the donor decay as judged by the reduced χ^2, the weighted residuals, and the autocorrelation of the residuals. Similar results were obtained for the $\bar{8}$ and $\overline{6'}$ isomers. The use of either a Gaussian or a Lorentzian model is only an approximation to the real system. The long tails of a Lorentzian model are due to the nature of the function and not due to the properties of the experimental system. The experimental decay curve could also be described by a superposition of two Gaussians (albeit more fitting parameters) to produce one distance distribution with the same mean distance and a slightly different shape without the long tails (Rice et al., 1991). Since one Gaussian model did not fit the decay curves at certain temperatures while a Lorentzian model fit all data sets, we used the latter throughout.

Previously, we used thermal perturbation to modulate the conformation of fluorescently labeled triantennary glycopeptides. Structural transitions were observed for the donor decay curves of **6** and **6'** when changing the temperature from 1 to 40 °C (Wu et al., 1991). A similar analysis of $\bar{8}$, $\bar{6}$, and $\overline{6'}$ at 1 and 40 °C illustrated only a systemic shift in the decay curve to shorter lifetimes (Figure 6).

The distance distribution for each temperature is shown in Figure 7. The donor–acceptor distance distribution of $\bar{8}$ demonstrates the same temperature dependency observed previously for **8**. However, $\bar{6}$ and $\overline{6'}$ possess a single distance population at all temperatures between 1 and 40 °C. The distance population for $\overline{6'}$ at 1 °C is slightly asymmetric, indicating that there may be a small fraction of the folded conformer. However, we cannot unambiguously ascertain its presence due to its small population (Figure 7C). This is in contrast to **6'** which displays the folded conformer as the major population at this temperature (Wu et al., 1991). Thus, temperature modulation failed to produce shorter donor–acceptor distance populations, indicating that the conformational dynamics of $\bar{6}$ and $\overline{6'}$ differ markedly from their substrates.

The donor decay for each product glycopeptide was also analyzed by eq 1 to obtain average lifetimes for the donor in the absence and presence of acceptor. The average lifetimes were then used to calculate average distances for each isomer at each temperature. Since the average lifetimes of the donor in the presence of acceptor were calculated independent of

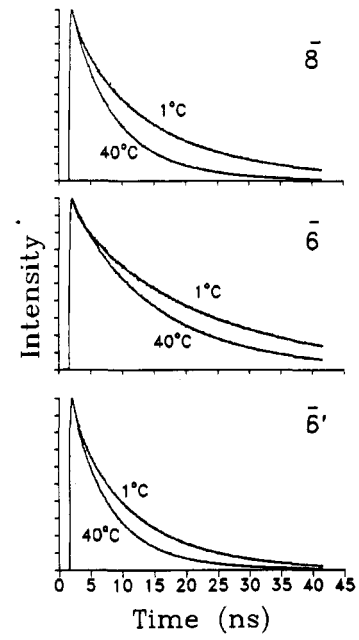

FIGURE 6: Influence of temperature on donor fluorescence decays. The donor decay curves for $\bar{8}$, $\bar{6}$, and $\overline{6'}$ are illustrated at 1 and 40 °C.

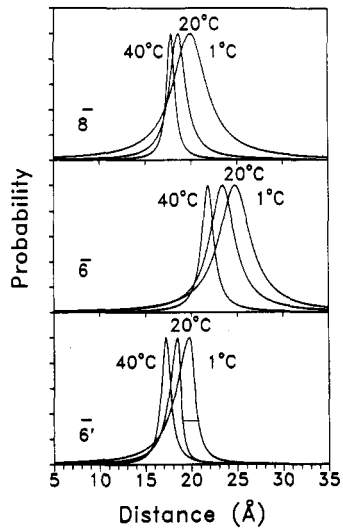

FIGURE 7: Distance distribution of $\bar{8}$, $\bar{6}$, and $\overline{6'}$ at three temperatures. The data were obtained from analysis of the donor decay using a Lorentzian model.

Table III: Average Distances[a] Calculated from Time-Resolved Data

T (°C)	**8**	$\bar{8}$	**6**	$\bar{6}$	**6'**	$\overline{6'}$
1	19.2	20.5	19.9	23.9	18.3	19.0
10	18.8		20.1		18.5	
20	18.5	19.3	20.2	23.1	18.3	18.2
30	18.0		20.0		18.0	
40	17.5	18.1	19.7	21.8	17.8	17.5
δr [b]	1.7	2.4	0.2	2.1	0.5	1.5

[a] Distances were calculated from average lifetimes at each temperature. Variation in the Förster distance was taken into account. Solution conditions were 2 mM phosphate, pH 7.2. [b] Difference in average distance from 1 to 40 °C.

the distance distribution analysis procedure, they provide additional comparisons between the triantennary glycopeptides and their respective exoglycosidase products. The results for glycopeptide products are shown in Table III, together with those calculated from the corresponding triantennary glycopeptide substrates (Wu et al., 1991). In the case of the

triantennary glycopeptides, the average distance is the overall average of one or two distance distributions. We observed that donor–acceptor distances became systematically shorter with increasing temperature, suggesting that higher temperatures cause increased intramolecular diffusion (Haas et al., 1978; Lakowicz et al., 1991), which was not included in our data analysis. The change in average distance ($\delta\bar{r}$) for **8** and $\bar{\mathbf{8}}$ is strongly influenced by the temperature between 1 and 40 °C. Also, the average distance for both $\bar{\mathbf{6}}$ and $\overline{\mathbf{6}'}$ is highly temperature dependent. This is in contrast to **6** and **6′**, whose average distance remains constant across this temperature range. Apparently, the extended and folded distance populations of **6** and **6′** compensate to provide the same overall average distance at each temperature whereas in $\bar{\mathbf{6}}$ and $\overline{\mathbf{6}'}$ there is no such compensation. As a result, the temperature-dependent decrease in the average distance for $\bar{\mathbf{8}}$ is comparable to that of $\overline{\mathbf{6}'}$ and $\bar{\mathbf{6}}$.

DISCUSSION

Using resonance energy-transfer techniques, we have investigated the conformation of a triantennary glycopeptide which serves as a ligand for the asialoglycoprotein receptor (Rice et al., 1990). The advantages of this technique include obtaining overall end-to-end distances in a single measurement, obtaining time-resolved measurements which quantify the degree of flexibility for individual antenna, and determining the thermodynamic energy barriers to molecular rotations by temperature modulation of the antenna conformation (Rice et al., 1991; Wu et al., 1991). In the present study, we have extended the energy-transfer studies by analyzing the conformation of three isomeric glycopeptides which retain only one of three branches.

The location of the fluorescent acceptor in the triantennary glycopeptide facilitated the generation of these unique glycopeptide probes (Figure 1, structures $\bar{\mathbf{8}}$, $\bar{\mathbf{6}}$, and $\overline{\mathbf{6}'}$.) The chromatographic and spectral data illustrate that following treatment of each triantennary isomer with β-galactosidase, β-*N*-acetylglucosaminidase, and α-mannosidase, the donor and acceptor fluorophores remain attached to the glycopeptide. The branch bearing the fluorescent probe is unaffected because β-galactosidase is incapable of removing a galactose residue which is modified with mono-*N*-dansylethylenediamine attached to the C-6 position, in agreement with other reports on the specificity of this enzyme (Distler & Jordian, 1973). During our studies, an α-mannosidase preparation from Boehringer Mannheim cleaved the oligosaccharide portion of $\overline{\mathbf{6}'}$, resulting in separation of the donor and acceptor fluorophores. We suspect this preparation contains an endomannosidase activity which is specific for the Manα1→6Man linkage that is unique to $\overline{\mathbf{6}'}$. Utilizing an α-mannosidase prepared by V-Labs circumvented this problem, resulting in the isolation of $\overline{\mathbf{6}'}$ containing both fluorophores.

The $\bar{\mathbf{8}}$, $\bar{\mathbf{6}}$, and $\overline{\mathbf{6}'}$ products were characterized by monosaccharide compositional analysis and proton NMR. Monosaccharide analysis agrees with the structure assigned to the products. Proton NMR revealed the presence of only three GlcNAc residues. The large chemical shifts introduced by the attachment of dansyl precluded assignment of all of the GlcNAc methyl and anomeric signals and the galactose anomeric signal. However, the Man 4 and 4′ anomeric resonances were unaffected by the exoglycosidase trimming and provided confirmatory data which agreed with our assignment of each isomer.

Steady-state energy-transfer experiments established that exoglycosidase trimming results in isomers with a similar donor–acceptor distance as compared with the triantennary glycopeptide substrates. Only a small decrease (approximately 1 Å) in the donor–acceptor distance was detected for each isomer.

Time-resolved energy-transfer experiments revealed a single donor–acceptor distance population for $\bar{\mathbf{6}}$, $\overline{\mathbf{6}'}$, and $\bar{\mathbf{8}}$ glycopeptides. This is in contrast to our previous studies which indicated two distinct donor–acceptor distance populations for **6** and **6′**, assigned as an extended and a folded conformation. The ratio of these two conformers was modulated by temperature (Rice et al., 1991; Wu et al., 1991).

These results may be rationalized if interantenna interactions play an important role in dictating the degree of antenna folding. Numerous laboratories have studied the flexibility of the Manα1–6Man linkage in high-mannose and complex oligosaccharides as well as their subfragments (Homans et al., 1986; Cumming et al., 1987; Mazurier et al., 1991). Molecular modeling studies indicate at least three low-energy conformations for the Man1–6Man linkage which arise from specific rotations around the Φ, Ψ, and Ω torsional angles. Recent evidence indicates that extension of the Manα1–6Man sequence with either a GlcNAcβ1–2 or an adjacent Manα1–3 linkage alters the number of low-energy conformers arising from this flexible linkage (Mazuerier et al., 1991). Homans et al. (1986) conclude that the flexibility of the Manα1–6Man linkge is sensitive to its intramolecular environment. In certain high-mannose and bisecting complex oligosaccharides, the linkage is held exclusively in a fixed folded-back conformation toward the core structure. However, complex oligosaccharides without a bisecting GlcNAc residue contained both a folded and an extended conformer for the Manα1–6Man linkage. Until recently, temperature modulation has not been utilized to investigate the degree of oligosaccharide flexibility. At 40 °C, the extension of the Manα1–6Man linkage is higly favored whereas at 0 °C a nearly equal ratio of extended and folded conformers exists (Wu et al., 1991). However, our present results demonstrate that trimming of the triantennary glycopeptide changes the environment of the Manα1–6Man linkage such that it is rigid at all temperatures between 0 and 40 °C.

Removal of two of the antennae eliminates the interaction which normally causes folding of the $\overline{\mathbf{6}'}$ antenna and provides a rigid glycopeptide structure. This explanation disputes the dogma which presumes that Manα1–6Man linkage are always highly flexible in solution (Imberty et al., 1990) and concurs with the results of Homans et al. that Manα1–6Man flexibility is modulated by neighboring residues (Homans et al., 1986).

A second site of flexibility was also implicated in our previous fluorescence energy-transfer studies on triantennary glycopeptide. Flexibility in the GlcNAcβ1–2Man linkage may account for the two conformers we observed for **6** and the nearly 2-fold greater temperature sensitivity of **6′** which also contains a GlcNAcβ1–2Man linkage. The loss of flexibility for both $\bar{\mathbf{6}}$ and $\bar{\mathbf{6}}$ as a result of trimming indicates that the flexibility of the GlcNAcβ1–2Man linkage is also modulated by neighboring sugar residues.

The results presented suggest that the extended conformations of $\bar{\mathbf{6}}$ and $\overline{\mathbf{6}'}$ are not only entropically favored but are also of lowest energy. We conclude that the flexibility of these two linkages in a triantennary glycopeptide is dictated by the oligosaccharide's primary structure in a similar way as the three-dimensional conformation of a protein is determined by the polypeptide sequence (Anfinsen, 1973). By trimming the oligosaccharide, we have removed those structural features which control the equilibrium between the

extended and folded conformers, even though the originally flexible glycosidic linkages remain unmodified. Future studies will need to address exactly which sugar residues on neighboring antenna contribute to folding of the oligosaccharide. These data may be obtained by analyzing each isomeric product during sequential exoglycosidase trimming.

Beyond demonstrating that oligosaccharide conformation is modified through exoglycosidases, our study points to potential problems in predicting the conformation of oligosaccharides based on data derived solely from short oligosaccharide fragments (Imberty et al., 1990). The data presented predict appreciable intramolecular interactions which may be difficult, if not impossible, to accurately account for when using computer modeling to build larger oligosaccharide structures from data acquired solely on disaccharides. In this way, fluorescence energy transfer may be considered as one of the very few techniques which can directly detect and quantify conformational heterogeneity in complex oligosaccharides. The use of fluorescence energy transfer in conjunction with exoglycosidase trimming may provide a detailed picture of the intramolecular interaction in complex oligosaccharides which dictate conformation and ultimately control biological specificity.

REFERENCES

Anfinsen, C. B. (1973) *Science 181*, 223–230.

Badea, M., & Brand, L. (1979) *Methods Enzymol. 61*, 378–425.

Bock, K., Arnarp, J., & Loenngren, J. (1982) *Eur. J. Biochem. 129*, 171–178.

Cumming, D. A., Shah, R. N., Krepinsky, J. J., Grey, A. A., & Carver, J. P. (1987) *Biochemistry 26*, 6655–6663.

Distler, J. J., & Jordian, G. W. (1973) *J. Biol. Chem. 248*, 6772–6780.

Edge, C. J., Singh, U. C., Bazzo, R., Taylor, G. L., Dwek, R. A., & Rademacher, T. W. (1990) *Biochemistry 29*, 1971–1974.

Grinvald, A., & Steinberg, I. Z. (1974) *Anal. Biochem. 59*, 583–598.

Haas, E., Katchalski-Katzir, E., & Steinberg, I. Z. (1978) *Biopolymers 17*, 11–31.

Hardy, M. R., Townsend, R. R., & Lee, Y. C. (1988) *Anal. Biochem. 170*, 54–62.

Homans, S. W. (1990) *Biochemistry 29*, 9110–9118.

Homans, S. W., Dwek, R. A., & Rademacher, T. W. (1987) *Biochemistry 26*, 6553–6560.

Imberty, A., Gerber, S., Tran, V., & Perez, S. (1990) *Glycoconjugate J. 7*, 27–54.

Kornfeld, R., & Kornfeld, S. (1985) *Annu. Rev. Biochem. 54*, 631–664.

Lakowicz, J. R., Kusba, J., Gryczynski, I., Wiczk, W., Szymacinski, J. H., & Johnson, M. L. (1991) *J. Phys. Chem. 95*, 9654–9660.

Lee, Y. C. (1989) *CIBA Found. Symp. 145*, 80–95.

Mazurier, J., Dauchezl, M., Vergoten, G., Montreuil, J., & Spik, G. (1991) *Glycoconjugate J. 8*, 390–399.

Poppe, L., Prill, R. S., Meyer, B., & Van Halbeek, H. (1992) *J. Biomol. NMR 2*, 109–136.

Rice, K. G., & Lee, Y. C. (1990) *J. Biol. Chem. 265*, 18423–18428.

Rice, K. G., & Lee, Y. C. (1992) *Adv. Enzymol. Relat. Areas Mol. Biol.* (1992) *66*, 41–83.

Rice, K. G., Weisz, O. A., Barthel, T., Lee, R. T., & Lee, Y. C. (1990) *J. Biol. Chem. 265*, 18429–18434.

Rice, K. G., Wu, P. G., Brand, L., & Lee, Y. C. (1991) *Biochemistry 30*, 6646–6655.

Rice, K. G., Takahashi, N., Namiki, Y., Tran, A. D., Lisi, P., & Lee, Y. C. (1992) *Anal. Biochem. 206*, 278–287.

Townsend, R. R., Hardy, M. R., Wong, T. C., & Lee, Y. C. (1986) *Biochemistry 25*, 5716–5725.

Wu, P. G., & Brand, L. (1992) *Biochemistry 31*, 7939–7947.

Wu, P. G., Rice, K. G., Brand, L., & Lee, Y. C. (1991) *Proc. Natl. Acad. Sci. U.S.A. 88*, 9355–9359.